Magnetic-field-driven quantum criticality of the Ising-class square lattice $Cr(dien)(O_2)_2 \cdot H_2O$ and the orientation dependence of its spin-flop transition

N. Kaur, J. H. Christian, J. S. Kinyon, V. Ramachandran, S. Nellutla, and N. S. Dalal*
Department of Chemistry and Biochemistry, Florida State University, Tallahassee, Florida 32306-4390, USA

Y. H. Kim and J. H. Park
National High Magnetic Field Laboratory, Tallahassee, Florida, 32310-3706, USA

C. Meehan and Y. Takano
Department of Physics, University of Florida, P.O. Box 118440, Gainesville, Florida 32611-8440, USA

(Received 16 March 2019; revised manuscript received 30 April 2019; published 25 June 2019)

The magnetic phase diagram of $Cr(dien)(O_2)_2 \cdot H_2O$ (dien $= C_4H_{13}N_3$), a quasi-two-dimensional spin-1 antiferromagnet known to exhibit quantum phase behavior, is reported. Specific heat, torque magnetometry, and magnetocalorimetry were employed to obtain the phase diagram down to 200 mK. Near the $T \rightarrow 0$ limit, the antiferromagnetic phase defers to a field-induced ferromagnetic phase at a critical field H_C. Analysis of the phase boundary through fitting with $(H - H_C) = \beta T^{\alpha}$ yielded H_C and the critical exponent α of the spin system. H_C and α were found to be 15.2 ± 0.02 T and 2.05 ± 0.09, respectively, when $\boldsymbol{H}$ is parallel to the easy magnetic axis, and 12.4 ± 0.01 T and 1.91 ± 0.06 when perpendicular to it. These critical exponents are indicative of an Ising-type spin system, which was an unanticipated result. Furthermore, torque magnetometry detected a spin-flop transition over a wide orientation range of nearly 70° in the *ab* plane. Mean field theory yielded an estimate of the long sought-after single-ion anisotropy for this compound, $D \approx 0.25$ K.

DOI: 10.1103/PhysRevB.99.214434

I. INTRODUCTION

The termination of a continuous phase transition line at zero temperature, i.e., a quantum critical point (QCP), results in the divergence of spatial and temporal parameters of quantum fluctuations that underlie quantum criticality and give rise to novel phenomena [1]. Quantum phase transitions occurring at the QCP are produced by tuning nonthermal parameters such as pressure, chemical composition, or magnetic field. The latter is perhaps the most convenient parameter since it is easily available in most laboratories. Low temperature studies near a QCP are used to investigate the dynamics of quantum fluctuations and help elucidate the origin of behavior for many quantum spin systems [2–10]. Since Hertz introduced quantum criticality in 1976 [2], there have been numerous experimental and theoretical studies on quantum critical behavior of condensed matter, with a large portion being performed on metals and atomic gases primarily belonging to the Heisenberg/XY class [11–14], many being spin dimers [15–17].

Low-dimensional antiferromagnets are attractive candidates for quantum criticality studies because their QCPs can be reached by applying a magnetic field at low temperatures. Additionally, enhanced quantum fluctuations can manifest if the system consists of ions with a small quantum spin [1]. During our search for new low-dimensional antiferromagnets, we focused on compounds that possess magnetic ions with an unusual oxidation state, as these sometimes exhibit novel or unexpected behavior, thus making them interesting systems for condensed matter research.

One such example is the rare oxidation state of Cr(IV) in $Cr(diethylenetriamine)(O_2)_2 \cdot H_2O$, (diethylenetriamine $= C_4H_{13}N_3$), hereafter Cr(dien) [18–22]. The core component of this compound has an elongated disk-shaped geometry as depicted in Fig. 1. Ramsey *et al.* had found a discrepancy regarding the anticipated temperature dependence of the two-dimensional (2D) antiferromagnetic transition T_N (Néel temperature) of this material under the influence of a magnetic field $\boldsymbol{H}$. Specific heat measurements showed that T_N fell to lower temperatures with increasing $\boldsymbol{H}$ from 0–6 T. However, a further increase in field caused an increase in T_N [20]. Generally, one expects T_N to decrease with the square of H [23], but an anomaly at 8 T seemed to indicate that T_N had reached a minimum point before increasing again. The source of this discrepancy was not understood, thus it seemed to be a worthwhile endeavor to map the magnetic phase diagram as a function of field.

Another reason for undertaking this study was to investigate the spin-flop phenomenon in Cr(dien), which to date remains unreported in the literature. Easy-axis antiferromagnets such as this often exhibit a spin-flop transition at T_{SF} when a magnetic field is applied parallel to the easy axis of magnetization while the system is in the antiferromagnetic state. This has been shown to often cause numerous physical irregularities and comprises the main features of spin reorientation [24–34]. A detailed investigation of the

*dalal@chem.fsu.edu

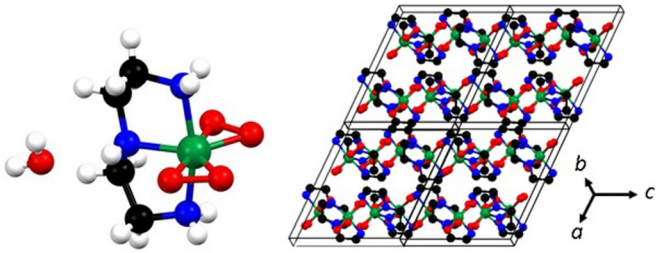

FIG. 1. Molecular structure and projection down the ***b*** axis of Cr(dien). Here green = chromium, red = oxygen, blue = nitrogen, black = carbon, and white = hydrogen.

angular dependence of the phase diagram seemed worthwhile, especially if the presence of a spin-flop transition could be shown.

Cr(dien) is a mononuclear, easy-axis, quasi-two-dimensional antiferromagnetic lattice with a total spin of $S = 1$ [20–22]. Furthermore, Cr(dien) is known [20] to crystallize in the monoclinic $C2/c$ space group with lattice parameters $a = 12.216$ Å, $b = 16.545$ Å, $c = 10.525$ Å, $\beta = 115.531°$, and $Z = 8$, as shown in Fig. 1. The magnetic ions form a square lattice along the *ac* plane, as illustrated in Fig. 2. A high-temperature series expansion based on the quadratic Hamiltonian in Eq. (2) had been previously used to estimate the exchange energies from susceptibility measurements. It was found that the ions are weakly coupled with $-J/k = 2.86$ K along the ***a*** axis and 2.88 K along the ***c*** axis. The spins order antiferromagnetically at $T_N = 2.55$ K in the absence of a magnetic field [20].

Herein, the result of specific heat, magnetocaloric effect, and magnetic torque experiments are used to construct the anisotropic magnetic phase diagram of Cr(dien) along both the ***b*** and ***c*** axes. In the $T \to 0$ temperature limit, the phase diagram is fit using the power law:

$$(H - H_C) = \beta T^{\alpha}. \tag{1}$$

Here H is the applied field, H_C is the critical field of a phase transition, T is the temperature of the phase transition, α is the critical exponent, and β is a constant of proportionality. The determination of the critical exponent in this power law is crucial since both the spin and spatial dimensions are vital elements of any spin model as can be seen in the following

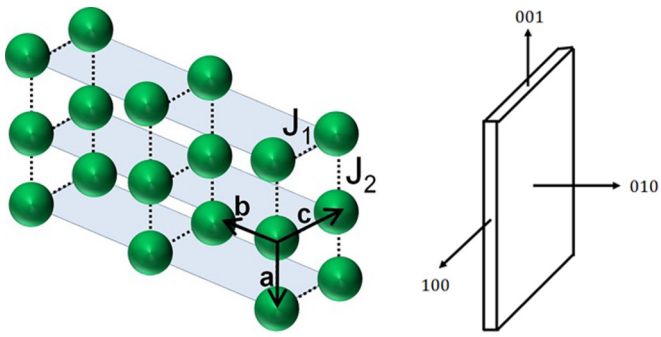

FIG. 2. Illustration of the magnetic network in Cr(dien), in which the magnetic ions are weakly coupled (J_1, J_2) in the *ac* plane. Additionally, crystal morphology is shown on the right.

magnetic Hamiltonian of an interacting spin system:

$$\mathcal{H} = \sum_{i,j} J_{ij}\mathbf{S_i} \cdot \mathbf{S_j} + \beta_e \mathbf{H} \cdot \boldsymbol{g} \cdot \mathbf{S} + D_z {S_z}^2. \tag{2}$$

The first sum (i, j) is representative of spin-spin interactions and often restricted to nearest neighbor interactions. When $J < 0$, interactions are considered antiferromagnetic, while values of $J > 0$ are indicative of ferromagnetic interactions. The second, Zeeman term includes the externally applied magnetic field $\boldsymbol{H}$, the anisotropic Landé g tensor, and the Bohr magneton β_e. The third term reflects the single-ion anisotropy D_z for a uniaxial system. The data obtained indicate that the saturation field of Cr(dien), i.e., the field when the antiferromagnetic phase defers to a paramagnetic (also called a field-induced ferromagnetic) phase, is strongly dependent on orientation and that the spin system belongs to the Ising class. We also show evidence of a spin-flop transition which is observed along many magnetic field orientations between ***b*** and ***c***.

II. EXPERIMENTAL METHODS

Single crystals of Cr(dien) were synthesized using a modified method by House and Garner [18]. Briefly, 5 g of $NaCr_2O_7 \cdot 2H_2O$ was dissolved in 6 ml of diethylenetriamine ($C_4H_{13}N_3$) and 40 ml of deinonized water. The solution was cooled in an ice bath, with the chromium reduced through the slow addition of 30% H_2O_2. The resulting solution was then allowed to evaporate at ambient temperature for 7 days, by which time dark brown crystals of approximately 0.3–1 cm length formed.

Specific heat and magnetocaloric effect were measured on single crystals of Cr(dien) using a homemade calorimeter, as described elsewhere [22] at the National High Magnetic Field Laboratory (NHMFL) in Tallahassee, FL. The measurements were performed using a ^{3}He/^{4}He dilution refrigerator in an 18 T superconducting magnet with the magnetic field applied along ***b*** and ***c*** separately. Specific heat was measured between 1.5 and 3.00 K with applied fields from 0–13.5 T. The magnetocaloric effect, i.e., the response of the temperature or entropy of a material to a change in the applied magnetic field, was measured between 200 mK and 2 K with applied fields from 10–15.5 T. Additional specific heat was measured between 1.8 and 4 K and 0–3 T using a Quantum Design Physical Property Measurement System (PPMS) that employs the time constant method [35].

Angular dependent torque magnetometry using a 0.002-in.-thick BeCu cantilever was used for additional temperature dependent measurements between 200 and 800 mK with applied fields from 0–15.5 T. In these measurements, a single crystal of Cr(dien) was placed on the rotatable cantilever inside a homogenous magnetic field. The sample was initially oriented with the magnetic field parallel to ***c*** and rotated incrementally until the applied field was parallel to ***b***. The torque of the sample was measured capacitively. Field homogeneity is vital in such measurements to ensure that the force experienced by the cantilever arises only from the torque generated by the sample. Under optimized conditions, this instrument can measure torque with a sensitivity $\approx 5 \times 10^{-13}$ N m.

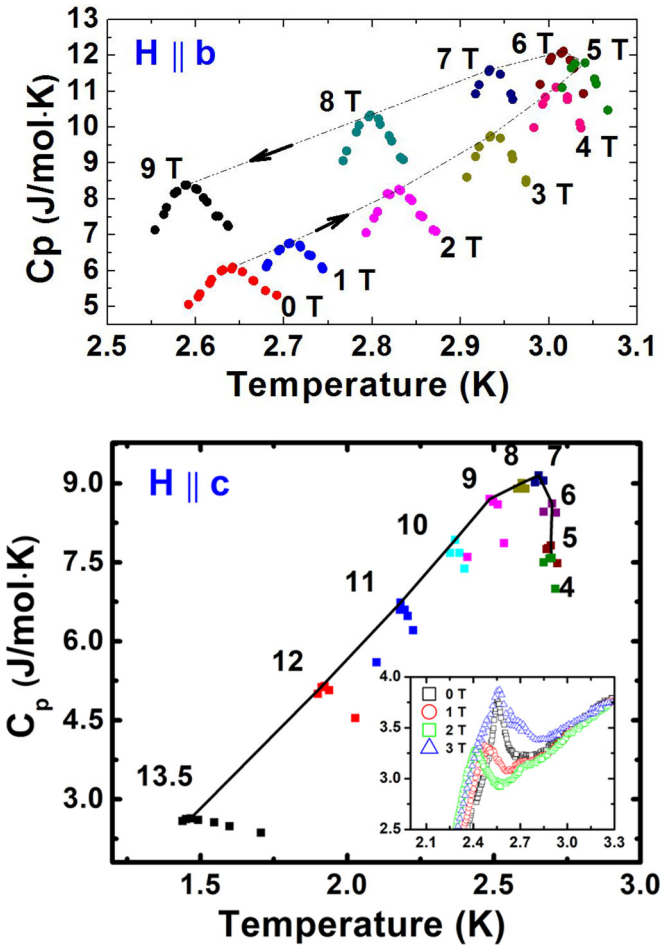

FIG. 3. Temperature dependence of the specific heat of Cr(dien) in applied magnetic fields ranging from 0–13.5 T along the ***b*** and ***c*** axes. The critical temperature of the transition corresponds to the peak in the C_p. The inset for the ***c*** direction depicts a wider temperature range for the peaks at 0–3 T in order to better represent the peak signature.

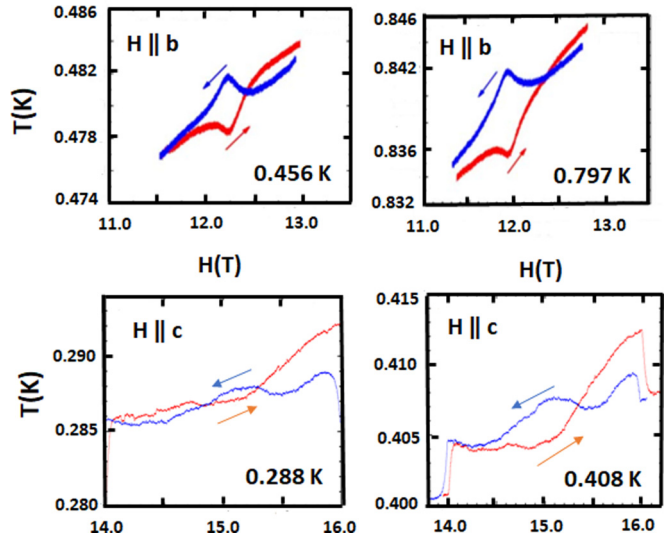

FIG. 4. Magnetocaloric measurements at 456 and 797 mK taken when $\boldsymbol{H} \parallel \boldsymbol{b}$ and at 288 and 408 mK when $\boldsymbol{H} \parallel \boldsymbol{c}$. The signature peak and dip are obtained by monitoring the sample temperature as a function of field and correspond with the paramagnetic to antiferromagnetic transition. Arrows indicate the field scan direction.

III. RESULTS AND DISCUSSION

A. Specific heat and magnetocaloric effect

The peaks observed in the specific heat (C_p) of Cr(dien) in Fig. 3 are indicative of the system's transition from a paramagnetic (PM) state into an antiferromagnetic (AF) one. In order to construct the magnetic phase diagram of Cr(dien) along the ***b*** and ***c*** axes separately, C_p was measured up to 13.5 T. As shown in Fig. 3, the λ-like peak becomes suppressed in its height, and its position is pushed to lower temperatures when $H > 4$ T. Below 4 T in the ***b*** orientation, the transition moves to higher temperatures as H is increased, while in the ***c*** orientation there exists a cusp in the transition temperature below 4 T. In summary, the transition temperatures were in good agreement with previous results [20]. Due to the suppression of the peak height at high fields, the position of the phase transition becomes difficult to identify, an occurrence indicating that the phase boundary between paramagnetic and antiferromagnetic states is becoming flat. For this reason, it is necessary to use the magnetocaloric effect to monitor the transition at high fields.

The magnetocaloric effect produced a peak and a dip indicative of a phase transition when sweeping the magnetic field upward and downward at a fixed temperature, respectively, as seen in Fig. 4. This asymmetry is expected for a continuous phase transition since the sample should exhibit heating when entering the ordered phase and cooling while leaving it. The transition field was obtained by averaging the peak and dip positions. Afterwards, the ordering temperatures and fields obtained from both C_p and magnetocaloric effect measurements were used to construct the magnetic phase diagram shown in Fig. 7.

B. Torque magnetometry and the spin-flop transition

The spin flop is a first order transition that occurs when the magnetic moments of a system flop perpendicular to the direction of the applied field in order to achieve a thermodynamically favored state [36]. Torque magnetometry is the ideal tool to probe for this type of transition since the torque exerted by the sample is proportional to the applied field and to the component of the magnetic dipole moment perpendicular to the field ($\boldsymbol{\tau} = \boldsymbol{\mu} \times \mathbf{H}$).

Both when $T < T_N = 2.5$ K and $H = 0$, Cr(dien) is in the antiferromagnetic state. Under such conditions, increasing ***H*** along ***c*** induces a spin-flop transition at a critical field H_{SF}, resulting in a sudden deflection of the cantilever holding the crystal and in turn producing an anomaly in the torque data. The spin flop was most evident when $\boldsymbol{H} \parallel \boldsymbol{c}$, becoming less pronounced when tilting the sample towards the *ab* plane. This observation led us to identify the ***c*** as the easy magnetic axis. As shown in Fig. 6, the transition was evident at all measured angles except 90°, although the transition becomes difficult to see past 70°. For this reason, it is convenient to view the first derivative of the torque data, which helps to better identify the transition. Specifically, the field for each

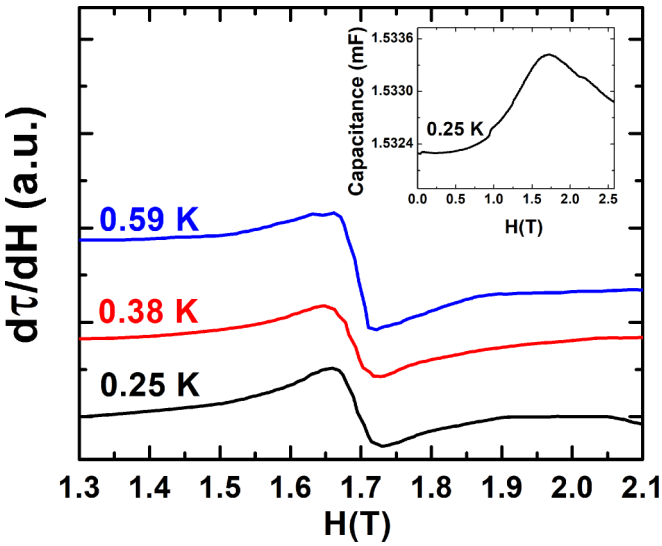

FIG. 5. The main figure displays the first derivative of the magnetic torque as a function of field. During these measurements $\boldsymbol{H}$ was fixed parallel to the $\boldsymbol{c}$ axis of Cr(dien) and swept at a fixed temperature in order to probe for the spin-flop transition; H_{SF} showed little variation with temperature. The inset shows the original peak at 0.25 K.

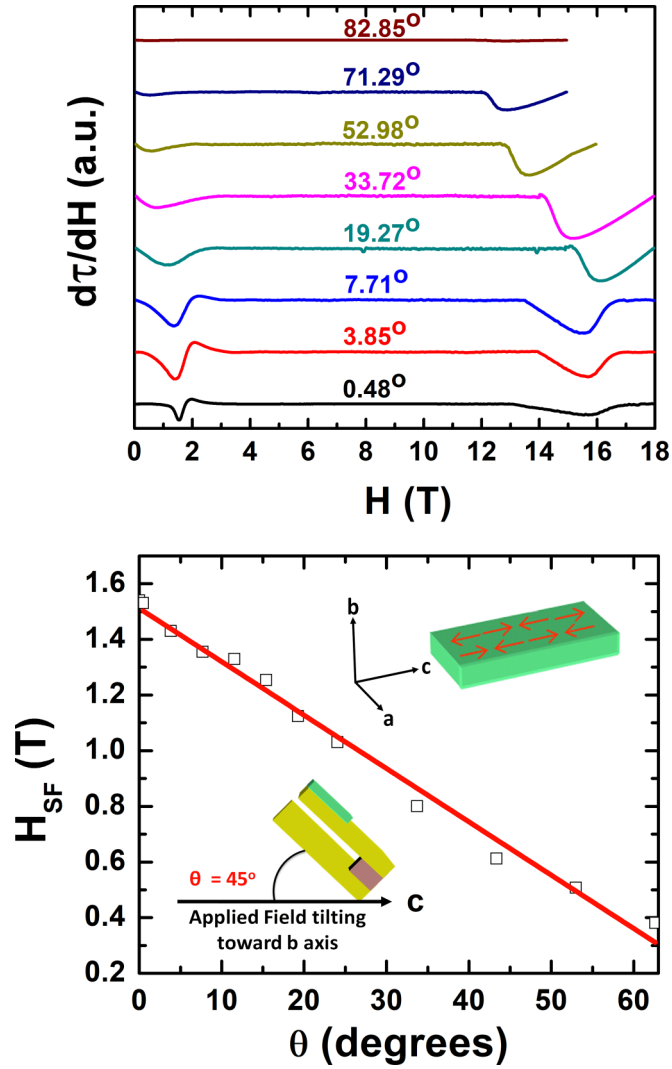

FIG. 6. The first derivative of the magnetic torque at different field orientations. When $\theta = 0°$, $\boldsymbol{H} \parallel \boldsymbol{c}$, while at 90°, $\boldsymbol{H} \parallel \boldsymbol{b}$. The low field signature marks the spin-flop transition, while the high field signature shows the transition to the paramagnetic phase. The angular dependence of H_{SF} is depicted on the bottom; angles above 70° are excluded from this plot because of the difficulty in identifying a precise value for H_{SF}.

associated temperature was identified by choosing the center of the peak-to-peak region of the derivative curve.

In order to map the critical field and temperature of the spin flop transition on the magnetic phase diagram, measurements of magnetic torque were obtained with a single crystal of Cr(dien) in a fixed position with $\boldsymbol{H}$ directly parallel to the easy $\boldsymbol{c}$ axis. As an example, the temperature and field dependence of the transition between 250 and 590 mK is depicted in Fig. 5. It is important to note that the magnetic field at which the transition occurred showed little variance within the studied temperature range of 250 mK to 2.3 K, keeping its extrapolated 0 K value of approximately 1.7 T. The magnetic torque data was used to add the individual H_{SF} values to the $\boldsymbol{H} \parallel \boldsymbol{c}$ phase diagram in Fig. 7.

Examination of the angular dependence of H_{SF} from Fig. 6 shows that it decreases in a somewhat linear manner with respect to θ, i.e., the critical field begins to decrease as the field is aligned closer with the *ab* plane. This stands in contrast to other studies on spin flop compounds such as $CaCo_2As_2$ [37] and Gd_5Ge_4 [38], which show a nonlinear increase in H_{SF} with respect to θ.

It seems worth noting that previous estimates have been made regarding the maximum angle Ψ at which H_{SF} can be observed for uniaxial antiferromagnets. Rohrer and Thomas found using a molecular field approximation that when the anisotropic intrasublattice exchange constant $K = 0$, $\Psi = 28.6° \times H_A/H_E$ [39]. Here H_E and H_A, respectively, refer to the exchange and uniaxial anisotropy fields. Using this formula with the values calculated in Sec. III D, $\Psi = 0.215/7.65 \times 28.6° \approx 1°$, which clearly contradicts our clear observation of the transition up to 70° towards the *ab* plane. This suggests that the Cr(dien) does not behave as a simple uniaxial antiferromagnet and that exchange constant K may play a greater role than was assumed, or that the classical mean-field theory may be insufficient for explaining the spin-flop behavior of this system. Regardless, a fundamental understanding of angular dependence of H_{SF} is lacking, and we hope that this study will stimulate further investigation.

C. Magnetic phase diagram

The magnetic phase diagram of Cr(dien) depicted in Fig. 7 clearly shows up to three different phases depending upon the orientation. Below T_N, for increasing $\boldsymbol{H}$ along $\boldsymbol{c}$, one crosses from the antiferromagnetic over to the spin-flop phase (AF-SF), followed by the spin-flop to the paramagnetic phase (SF-PM). On the other hand, increasing the temperature when $H < H_{SF}$ allows one to cross from the antiferromagnetic to paramagnetic phase (AF-PM). All three phases meet at a

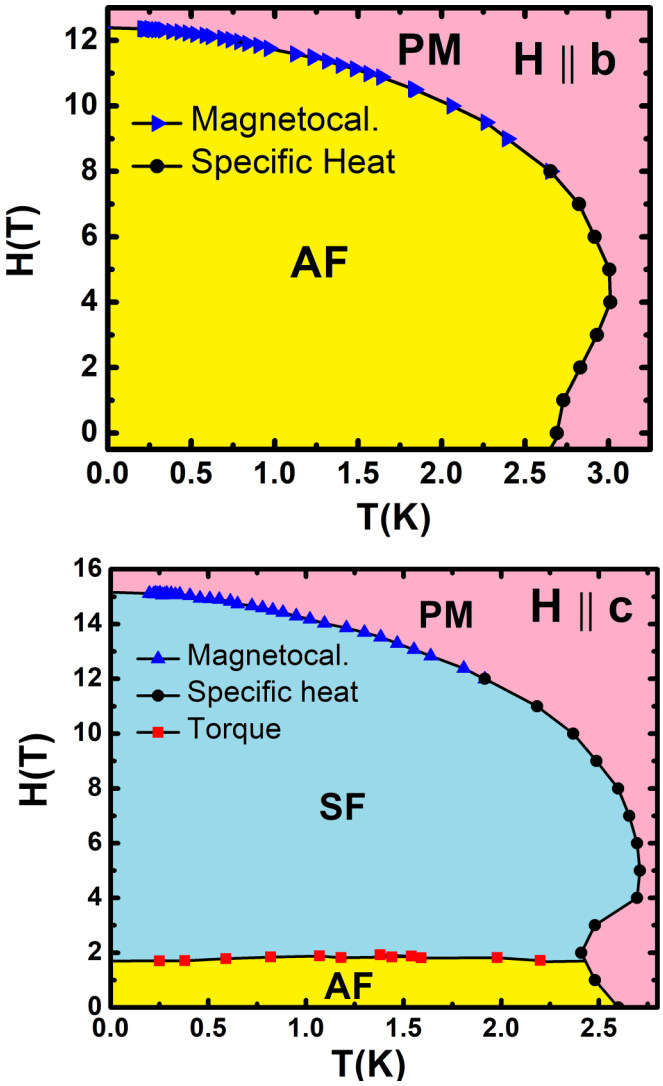

FIG. 7. Magnetic phase diagrams of Cr(dien) with the field applied along the crystallographic ***b*** and ***c*** axes. As expected, no spin-flop transition could be found on the perpendicular ***b*** axis.

bifurcation point $T_{\rm bif}$. When $\boldsymbol{H} \perp \boldsymbol{c}$, there is no spin flop, and hence only two phases and a corresponding AF-PM curve.

The magnetic properties exhibit a very strong orientation dependence. Besides the spin-flop transition, it is worth noting that the $\boldsymbol{H} \parallel \boldsymbol{c}$ orientation exhibits a higher saturation field $H_{\rm sat}$ than when $\boldsymbol{H} \parallel \boldsymbol{b}$. It seems unlikely that the inclusion of exchange anisotropy would make the saturation field anisotropic [40]. However, a field-dependent single ion anisotropy term in the Hamiltonian $D_z {S_z}^2$ could perhaps account for the orientation dependence of the saturation field [41]. For small fields, this may be approximated as

$$D_{\rm eff}(H) = D_z - \frac{1}{2}(\chi_\perp - \chi_\parallel){H_z}^2 \tag{3a}$$

$$= 1 - \frac{{H_z}^2}{H_{\rm SF}^2}. \tag{3b}$$

Here H_z refers to the magnetic field applied along the the z axis of anisotropy. With this perspective, it can be seen that when $H_z = H_{\rm SF}$, the Zeeman energy overcomes the anisotropy and allows the spins to flop to the perpendicular plane. Generally, $D_{\rm eff}(H)$ is usually independent of temperature [41], as $D(T)$ and $[\chi_\perp(T) - \chi_\parallel(T)]$ often have similar temperature dependencies, though there are exceptions as K_2MnF_4, which is manifested when the (AF-SF) curve is not completely horizontal [42]. We would like to point out that Cr(diene) shows a slight negative slope at low temperatures, with $H_{\rm SF}$ ranging from 1.7–1.9 T. Regardless, the introduction of the effective field-dependent anisotropy essentially allows Eq. (2) to be treated as an effective Hamiltonian such that

$$\mathcal{H} = \sum_{i,j} J_{ij}\mathbf{S_i} \cdot \mathbf{S_j} + D_{\rm eff}(H){S_z}^2. \tag{4}$$

This model allows one to arrive at the well-known result that for classical spins on a square lattice $g\beta_e H_{\rm sat} = 2S(4J - D)$ when $\boldsymbol{H} \parallel z$ and $g\beta_e H_{\rm sat} = 2S(4J + D)$ when $\boldsymbol{H} \perp z$, where z refers to the axis of anisotropy [41,43]. Since the saturation field is largest in the ***c*** direction, that in which there is a clear spin-flop transition, it would be necessary for $D < 0$, that is for us to assign a hard-axis anisotropy onto this system. Here the hard axis should be aligned with the crystallographic ***b*** axis. In this direction, the saturation field is lower, and the spin-flop transition is either absent or experimentally very hard to see.

In addition to the saturation field, the introduction of D_z term is also quite useful for describing the general shape of the phase diagram, which has also been used with great success for $Mn(HCOO)_2 \cdot 2H_2O$ [44], K_2MnF_4 [42], and Rb_2MnCl_4 [45]. Specifically, it much resembles that of a 2D isotropic Heisenberg antiferromagnet with a weak field-dependent anisotropy. The phase diagram has already been extensively detailed [41,46], but some features are worth highlighting here. The AF region is generally of Ising character, and the SF region is best described as having an XY-like low temperature phase.

Additionally, the high-field curve (SF-PM) near $T = 0$ actually mimics that of a Berezinsky-Kosterlitz-Thouless (BKT) transition because of the degeneracy of a canted spin-flop ground state; it is important to emphasize that the underlying BKT transition does not arise from a classic 2D Heisenberg model, but from the XY-type behavior instigated by the D_z term [47]. The spin correlation is expected to decay with a power law according to Eq. (1) with $0 < T_{\rm C} < T_{\rm XY}$, $T_{\rm XY}$ being the BKT transition of a pure 2D XY system. When $\boldsymbol{H} \perp \boldsymbol{D}_z$, the AF region is of Ising character, and there is no SF transition; T_C will slowly increase with H and only start to bend back towards $T = 0$ once magnetic saturation effects become important, that is once H approaches H_E.

One important difference between the experimental phase diagram of Cr(diene) and the theoretically predicted one lies in the shape of the cusp when $\boldsymbol{H} \parallel \boldsymbol{c}$. Theoretically, the cusp region is expected to be much sharper as one approaches $T_{\rm bif}$ for an axial system [41,46]. However, interplanar antiferromagnetic interactions, represented by a D_x term in the Hamiltonian, have been shown to theoretically soften the edges near the cusp [41]. In this case, $T_{\rm bif}$ is essentially described as a BKT-type transition, with its precise value $0 < T_{\rm bif} < T_{\rm XY}$ depending upon the relative strength of the interplanar interactions. It can also be argued that there is a random-field effect at work here that comes from crystal

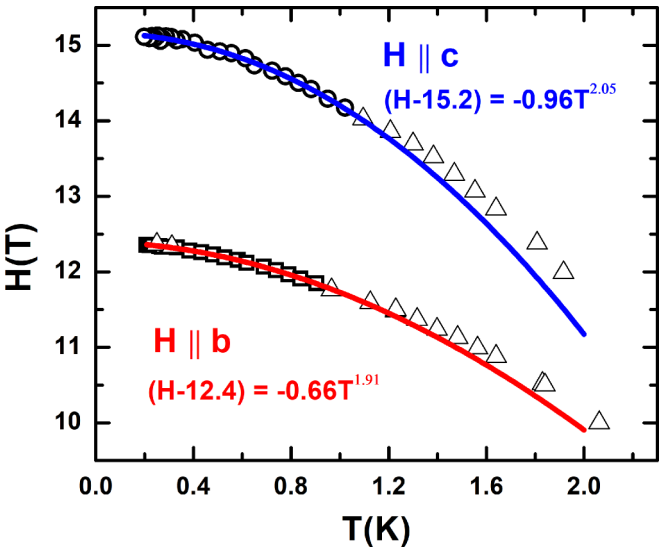

FIG. 8. A power-law fitting of select low temperature data points taken from the magnetic phase diagram when $\boldsymbol{H} \parallel \boldsymbol{b}$ (squares, red) and $\boldsymbol{c}$ (circles, blue) axes. The additional triangles are data points not used in the power-law fitting, which starts to break down at higher temperatures. The equation is depicted near each fit.

defects, analogous to what has been suggested as an impurity effect in mixed crystals such as $Fe_{0.725}Co_{0.275}Cl_2$ [48] and $Mn_xZn_{1-x}F_2$ [49].

A standard nonlinear curve fitting algorithm from origin 8.5 was used to determine the QCP, i.e., the critical field H_C and the critical exponent α, the result of which can be seen in Fig. 8. Application of $\boldsymbol{H} \parallel \boldsymbol{c}$ yielded $H_C = 15.2 \pm 0.02$ T and $\alpha = 2.05 \pm 0.09$, while $\boldsymbol{H} \parallel \boldsymbol{b}$ yielded $H_C = 12.4 \pm 0.01$ T and $\alpha = 1.91 \pm 0.06$. These critical exponents are higher than those observed for Heisenberg/XY models and are characteristic of the Ising universality class [50–52]. This observation shows that care should be given with regards to classifying what we call the SF phase. Rotating Cr(diene) from the AF phase along $\boldsymbol{b}$ to the SF phase along $\boldsymbol{c}$ should by definition bring the spins from an Ising to XY symmetry, yet the critical exponents indicate otherwise [53]. To our knowledge, this is the first documented case of an experimentally determined α for a $S = 1$ square lattice antiferromagnetic system.

D. Estimation of *D*

Many attempts have been made to obtain an EPR signal from Cr(diene) using frequencies of 9.5–400 GHz and temperatures of 1.8–400 K, as it is the most direct means of measuring single-ion anisotropy D, also known as zero-field splitting. Unfortunately, no signal could be detected, possibly due to the magnitude of D or the spin-lattice relaxation time τ_1. In order to clarify this point, we thought it prudent to use the well-known mean field molecular theory [23,36] as a means of estimating D from the extrapolated value of H_{SF} and H_C at $T = 0$ when $\boldsymbol{H} \parallel \boldsymbol{c}$. The equations governing this relationship are given below:

$$H_{SF} = \sqrt{2H_E H_A - {H_A}^2}, \tag{5a}$$

$$H_C = 2H_E - H_A, \tag{5b}$$

$$H_A = 2|D|(S - 1/2)(g\mu_B)^{-1}, \tag{5c}$$

$$H_E = 2z|J|S(g\mu_B)^{-1}. \tag{5d}$$

Here z is the coordination number of the magnetic ion, and J is the isotropic intramolecular coupling constant. It is assumed that the Cr(IV) ion is the sole contributor to the anisotropy field and that any J anisotropy is negligible. From Eq. (5) it can be shown that $H_E = (H_{SF}^2 + H_C^2)/2H_C$. Taking $H_C = 15.2$ T from the power-law fit and $H_{SF} = 1.7$ T, one finds $H_E \approx 7.7$ T, and by extension $H_A \approx 0.19$ T. Using the $g_c = 1.96$ obtained from Ramsey *et al.* [20] and $z = 4$, it was found that $|D| \approx 0.25$ K and $|J| \approx 1.3$ K. Here J is in fair agreement with what was found by Ramsey via susceptibility fitting. Additionally, the small magnitude of D relative to nearest neighbor interactions suggest that the single-ion anisotropy is not responsible for the EPR silence. Rather, a long τ_1 and the associated spin saturation is likely the reason, as no signal could be observed, even at low temperatures.

IV. CONCLUSIONS

We report the magnetic phase diagram of $Cr(dien)(O_2)_2 \cdot H_2O$ and the orientation dependence of its spin-flop transition obtained through specific heat, torque magnetometry, and magnetocalorimetry using temperatures down to 200 mK and applied fields from 0–16 T. It was found for all orientations that as $T \to 0$, the antiferromagnetic phase defers to a PM, that is a field-induced ferromagnetic phase at a critical field H_C according to the power law given by Eq. (1). When $\boldsymbol{H}$ is aligned with the magnetic easy axis, i.e., the crystallographic $\boldsymbol{c}$ axis, H_C and the critical exponent α are, respectively, 15.2 ± 0.02 T and 2.05 ± 0.09. On the other hand, when $\boldsymbol{H}$ is applied along the hard axes, i.e., the $\boldsymbol{b}$ axis, the values are 12.4 ± 0.01 T and 1.91 ± 0.06. Such critical exponents are indicative of an Ising type spin system, which is quite unexpected for a square lattice. The reason for the cusp, or deviation from the power-law type behavior visible in the phase diagram is currently attributed to either interplanar antiferromagnetic interactions or random-field effect introduced by lattice defects.

Additionally, torque magnetometry measurements allowed for the detection of a nearly temperature independent spin flop transition H_{SF} at 1.7 T along the crystallographic $\boldsymbol{c}$ axis. Surprisingly this remained detectable for nearly $\theta = 70^\circ$ into the ab plane, with H_{SF} decreasing linearly with respect to θ. Our attempts at modeling the unusually large range of spin-flop behavior proved to be unsuccessful, with the origin of this observation remaining unclear. Additionally, since the SF phase is expected to have XY symmetry, indication of Ising criticality through the α values is quite surprising. Finally, mean field theory allowed for an estimate of the zero-field single-ion anisotropy that remained undetectable with EPR, $D \approx 0.25$ K.

ACKNOWLEDGMENTS

A large portion of this work was carried out at the National High Magnetic Field Laboratory (NHMFL), which is supported by the National Science Foundation (NSF) via Cooperative Agreement DMR-1157490 and the State of Florida.

[1] S. Sachdev, *Quantum Phase Transitions*, 2nd ed. (Cambridge University Press, Cambridge, 2011).

[2] J. A. Hertz, Quantum critical phenomena, Phys. Rev. B **14**, 1165 (1976).

[3] H. v. Löhneysen, A. Rosch, M. Vojta, and P. Wölfle, Fermi-liquid instabilities at magnetic quantum phase transitions, Rev. Mod. Phys. **79**, 1015 (2007).

[4] P. Gegenwart, Q. Si, and F. Steglich, Quantum criticality in heavy-fermion metals, Nat. Phys. **4**, 186 (2008).

[5] N. D. Mathur, F. M. Grosche, S. R. Julian, I. R. Walker, D. M. Freye, R. K. W. Haselwimmer, and G. G. Lonzarich, Magnetically mediated superconductivity in heavy fermion compounds, Nature (London) **394**, 39 (1998).

[6] H. Q. Yuan, F. M. Grosche, M. Deppe, C. Geibel, G. Sparn, and F. Steglich, Observation of two distinct superconducting phases in $CeCu_2Si_2$, Science **302**, 2104 (2003).

[7] E. Fradkin and S. A. Kivelson, Liquid-crystal phases of quantum Hall systems, Phys. Rev. B **59**, 8065 (1999).

[8] M. P. Lilly, K. B. Cooper, J. P. Eisenstein, L. N. Pfeiffer, and K. W. West, Evidence for an Anisotropic State of Two-Dimensional Electrons in High Landau Levels, Phys. Rev. Lett. **82**, 394 (1999).

[9] R. A. Borzi, S. A. Grigera, J. Farrell, R. S. Perry, S. J. S. Lister, S. L. Lee, D. A. Tennant, Y. Maeno, and A. P. Mackenzie, Formation of a nematic fluid at high fields in $Sr_3Ru_2O_7$, Science **315**, 214 (2007).

[10] Y. S. Oh, K. H. Kim, P. A. Sharma, N. Harrison, H. Amitsuka, and J. A. Mydosh, Interplay Between Fermi Surface Topology and Ordering in URu_2Si_2 Revealed Through Abrupt Hall Coefficient Changes in Strong Magnetic Fields, Phys. Rev. Lett. **98**, 016401 (2007).

[11] M. Greiner, C. A. Regal, and D. S. Jin, Emergence of a molecular Bose-Einstein condensate from a Fermi gas, Nature (London) **426**, 537 (2003).

[12] M. H. Anderson, J. R. Ensher, M. R. Matthews, C. E. Wieman, and E. A. Cornell, Observation of Bose-Einstein condensation in a dilute atomic vapor, Science **269**, 198 (1995).

[13] F. Schreck, L. Khaykovich, K. L. Corwin, G. Ferrari, T. Bourdel, J. Cubizolles, and C. Salomon, Quasipure Bose-Einstein Condensate Immersed in a Fermi Sea, Phys. Rev. Lett. **87**, 080403 (2001).

[14] K. B. Davis, M. O. Mewes, M. R. Andrews, N. J. van Druten, D. S. Durfee, D. M. Kurn, and W. Ketterle, Bose-Einstein Condensation in a Gas of Sodium Atoms, Phys. Rev. Lett. **75**, 3969 (1995).

[15] N. Kawashima, Quantum critical point of the XY model and condensation of field-induced quasiparticles in dimer compounds, J. Phys. Soc. Jpn. **73**, 3219 (2004).

[16] S. E. Sebastian, N. Harrison, C. D. Batista, L. Balicas, M. Jaime, P. A. Sharma, N. Kawashima, and I. R. Fisher, Dimensional reduction at a quantum critical point, Nature (London) **441**, 617 (2006).

[17] D. Poilblanc, M. Mambrini, and D. Schwandt, Effective quantum dimer model for the Kagome Heisenberg antiferromagnet: Nearby quantum critical point and hidden degeneracy, Phys. Rev. B **81**, 180402(R) (2010).

[18] D. A. House and C. S. Garner, Diperoxodiethylenetriamminechromium(IV) 1-hydrate: A new chromium(IV)peroxo compound, Nature (London) **208**, 776 (1965).

[19] D. A. House and C. S. Garner, The use of chromium(IV) diperoxo amines in the synthesis of chromium(III) amine complexes. I. Some monoethylenediamine and monodiethylenetriamine complexes, Inorg. Chem. **5**, 840 (1966).

[20] C. M. Ramsey, B. Cage, P. Nguyen, K. A. Abboud, and N. S. Dalal, Ligand dependence of magnetic dimensionality in chromium(IV) complexes: Layered vs three-dimensional antiferromagnets, Chem. Mater. **15**, 92 (2003).

[21] B. Cage, R. Leniek, and N. Dalal, Novel magnetic and heat capacity properties of the Cr(IV) diperoxides, J. Appl. Phys. **87**, 6010 (2000).

[22] Y. H. Kim, N. Kaur, B. M. Atkins, N. S. Dalal, and Y. Takano, Fluctuation-Induced Heat Release from Temperature-Quenched Nuclear Spins Near a Quantum Critical Point, Phys. Rev. Lett. **103**, 247201 (2009).

[23] L. de Jongh and A. Miedema, Experiments on simple magnetic model systems, Adv. Phys. **23**, 1 (1974).

[24] N. J. Poulis, J. van den Handel, J. Ubbink, J. A. Poulis, and C. J. Gorter, On antiferromagnetism in a single crystal, Phys. Rev. **82**, 552 (1951).

[25] N. Poulis and G. Hardeman, Behaviour of a single crystal of $CuCl_2 \cdot 2H_2O$ near the néel temperature, Physica **18**, 429 (1952).

[26] C. J. Gorter, Observations on antiferromagnetic $CuCl_2 \cdot 2H_2O$ crystals, Rev. Mod. Phys. **25**, 332 (1953).

[27] J. W. Lynn, P. Heller, and N. A. Lurie, Neutron-diffraction study of the staggered magnetization of $CuCl_2 \cdot 2D_2O$, Phys. Rev. B **16**, 5032 (1977).

[28] G. K. Chepurnykh, Ground state of an antiferromagnet in a magnetic field of arbitrary direction, Fiz. Tverd. Tela (Leningrad) **10**, 1917 (1968).

[29] A. N. Bogdanov and V. T. Telepa, Basic state of easy-axis antiferromagnet in an oblique field, Fiz. Tverd. Tela (Leningrad) **24**, 2420 (1982) [Sov. Phys. Solid State **24**, 1374 (1982)].

[30] V. G. Baryakhtar, A. N. Bogdanov, V. T. Telepa, and D. A. Yablonskii, Domain-structure theory of antiferromagnets in the intermediate phase at spin-flop transition, Fiz. Tverd. Tela (Leningrad) **26**, 389 (1984) [Sov. Phys. Solid State **26**, 231 (1984)].

[31] V. G. Baryakhtar, A. E. Borovik, and V. A. Popov, Theory of intermediate states of an antiferromagnet during a first-order phase transition in an external magnetic field, JETP Lett. **9**, 391 (1969).

[32] K. L. Dudko, V. V. Eremenko, and V. M. Fridman, Magnetic stratification during flipping of antiferromagnetic manganese fluoride sublattices, Zh. Eksp. Teor. Fiz. **61**, 678 (1971) [Sov. Phys. JETP **34**, 362 (1972)].

[33] A. R. King and D. Paquette, Spin-Flop Domains in MnF_2, Phys. Rev. Lett. **30**, 662 (1973).

[34] D. L. Mills, Surface Spin-Flop State in a Simple Antiferromagnet, Phys. Rev. Lett. **20**, 18 (1968).

[35] G. R. Stewart, Measurement of low temperature specific heat, Rev. Sci. Instrum. **54**, 1 (1983).

[36] R. L. Carlin, *Magnetochemistry*, 1986th ed. (Springer, New York, 2011).

[37] W. Zhang, K. Nadeem, H. Xiao, R. Yang, B. Xu, H. Yang, and X. G. Qiu, Spin-flop transition and magnetic phase diagram in $CaCo_2As_2$ revealed by torque measurements, Phys. Rev. B **92**, 144416 (2015).

[38] Z. W. Ouyang, V. K. Pecharsky, K. A. Gschneidner, D. L. Schlagel, and T. A. Lograsso, Angular dependence of the spin-flop transition and a possible structure of the spin-flop phase of Gd_5Ge_4, Phys. Rev. B **76**, 134415 (2007).

[39] H. Rohrer and H. Thomas, Phase transitions in the uniaxial antiferromagnet, J. Appl. Phys. **40**, 1025 (1969).

[40] A. Berkowitz and K. Takano, Exchange anisotropy: A review, J. Magn. Magn. Mater. **200**, 552 (1999).

[41] H. D. Groot and L. D. Jongh, Phase diagrams of weakly anisotropic Heisenberg antiferromagnets, nonlinear excitations (solitons) and random-field effects, Physica B+C **141**, 1 (1986).

[42] L. J. de Jongh, L. P. Regnault, J. Rossat Mignod, and J. Y. Henry, Field dependent neutron scattering study of the quasi 2D Heisenberg antiferromagnet K_2MnF_4, J. Appl. Phys. **53**, 7963 (1982).

[43] B. Costa and A. Pires, Phase diagrams of a two-dimensional Heisenberg antiferromagnet with single-ion anisotropy, J. Magn. Magn. Mater. **262**, 316 (2003).

[44] J. Schutter, J. Metselaar, and D. D. Klerk, The magnetic diagram of state of manganese formate dihydrate, Physica **61**, 250 (1972).

[45] H. Rauh, W. A. C. Erkelens, L. P. Regnault, J. Rossat-Mignod, W. Kullman, and R. Geick, Magnetic phase diagram of Rb_2MnCl_4, a quasi-two-dimensional uniaxial antiferromagnet, J. Phys. C: Solid State Phys. **19**, 4503 (1986).

[46] D. P. Landau and K. Binder, Phase diagrams and critical behavior of a two-dimensional anisotropic Heisenberg antiferromagnet, Phys. Rev. B **24**, 1391 (1981).

[47] J. Kosterlitz and D. Thouless, in *Chapter 5 Two-Dimensional Physics*, edited by D.F. Brewer, Progress in Low Temperature Physics Vol. 7 (Elsevier, New York, 1978), pp. 371–433.

[48] P.-z. Wong and J. W. Cable, Observation of a disordered spin-flop phase in $Fe_{0.725}Co_{0.275}Cl_2$, Phys. Rev. B **30**, 485 (1984).

[49] Y. Shapira, Phase diagrams of pure and diluted low anisotropy antiferromagnets: Crossover effects (invited), J. Appl. Phys. **57**, 3268 (1985).

[50] S. E. Sebastian, V. S. Zapf, N. Harrison, C. D. Batista, P. A. Sharma, M. Jaime, I. R. Fisher, and A. Lacerda, Comment on Bose-Einstein Condensation of Magnons in Cs_2CuCl_4, Phys. Rev. Lett. **96**, 189703 (2006).

[51] C. J. Hamer, J. Oitmaa, Z. Weihong, and R. H. McKenzie, Critical behavior of one-particle spectral weights in the transverse Ising model, Phys. Rev. B **74**, 060402(R) (2006).

[52] S. Nellutla, M. Pati, Y.-J. Jo, H. D. Zhou, B. H. Moon, D. M. Pajerowski, Y. Yoshida, J. A. Janik, L. Balicas, Y. Lee, M. W. Meisel, Y. Takano, C. R. Wiebe, and N. S. Dalal, Magnetic field induced quantum phase transition of the $s = \frac{1}{2}$ antiferromagnet K_2NaCrO_8, Phys. Rev. B **81**, 064431 (2010).

[53] We would like to thank a reviewer for raising this point.